Functional Toll-like Receptor 4 Overexpression in Papillary Thyroid Cancer by MAPK/ERK-induced ETS1 Transcriptional Activity

Victoria Peyret[1], Magalí Nazar[1], Mariano Martín[1], Amado A. Quintar[2], Elmer A. Fernandez[3], Romina C. Geysels[1], Cesar S. Fuziwara[4], María M. Montesinos[1], Cristina A. Maldonado[2], Pilar Santisteban[5], Edna T. Kimura[4], Claudia G. Pellizas[1], Juan P. Nicola[1]*, Ana M. Masini-Repiso[1]*

[1] Centro de Investigaciones en Bioquímica Clínica e Inmunología - Consejo Nacional de Investigaciones Científicas y Técnicas. Departamento de Bioquímica Clínica, Facultad de Ciencias Químicas, Universidad Nacional de Córdoba, Córdoba, Argentina.

[2] Instituto de Investigaciones en Ciencias de la Salud - Consejo Nacional de Investigaciones Científicas y Técnicas. Centro de Microscopía Electrónica, Facultad de Ciencias Médicas, Universidad Nacional de Córdoba, Córdoba, Argentina.

[3] Centro de Investigaciones y Desarrollo en Inmunología y Enfermedades Infecciosas - Consejo Nacional de Investigaciones Científicas y Técnicas, Universidad Católica de Córdoba and Facultad de Ciencias Exactas, Físicas y Naturales, Universidad Nacional de Córdoba, Córdoba, Argentina.

[4] Department of Cell and Developmental Biology, Institute of Biomedical Sciences, University of São Paulo, São Paulo, Brazil.

[5] Instituto de Investigaciones Biomédicas Alberto Sols - Consejo Superior de Investigaciones Científicas, Universidad Autónoma de Madrid and Centro de Investigación Biomédica en Red Cáncer (CIBERONC), Instituto de Salud Carlos III, Madrid, Spain.

* These authors contributed equally to this work and should be considered as co-corresponding authors.

ABBREVIATED TITLE: TLR4 Overexpression in Thyroid Cancer

ABBREVIATION LIST: Toll-like receptors (TLRs), Lipopolysaccharide (LPS), Nuclear factor-κB (NF-κB), Mitogen-activated protein kinase (MAPK), Extracellular signal-regulated kinase (ERK), E26 transformation-specific (ETS), The Cancer Genome Atlas (TCGA), Gene Expression Omnibus (GEO).

CO-CORRESPONDING AUTHORS: Dr. Juan Pablo Nicola (jpnicola@fcq.unc.edu.ar) and Dr. Ana María Masini-Repiso (amasini@fcq.unc.edu.ar). Centro de Investigaciones en Bioquímica Clínica e Inmunología - Consejo Nacional de Investigaciones Científicas y Técnicas. Departamento de Bioquímica Clínica, Facultad de Ciencias Químicas, Universidad Nacional de Córdoba. Haya de la Torre y Medina Allende, 5000 Córdoba, Argentina. Phone: +54 0351 535-3851.

CONFLICT OF INTEREST STATEMENT: The authors have nothing to disclose.

ABSTRACT

Emerging evidence suggests that unregulated Toll-like receptors (TLRs) signaling promotes tumor survival signals, thus favoring tumor progression. Here, the mechanism underlying TLR4 overexpression in papillary thyroid carcinomas (PTCs) mainly harboring the $BRAF^{V600E}$ mutation was studied. TLR4 was overexpressed in PTCs compared to non-neoplastic thyroid tissue. Moreover, paired clinical specimens of primary PTC and its lymph node metastasis showed a significant upregulation of TLR4 levels in the metastatic tissues. In agreement, conditional $BRAF^{V600E}$ expression in normal rat thyroid cells and mouse thyroid tissue upregulated TLR4 expression levels. Furthermore, functional TLR4 expression was demonstrated in PTC cells by increased NF-κB transcriptional activity in response to the exogenous TLR4-agonist lipopolysaccharide (LPS). Of note, The Cancer Genome Atlas (TCGA) data analysis revealed that $BRAF^{V600E}$-positive tumors with high TLR4 expression were associated with shorter disease-free survival. Transcriptomic data analysis indicated a positive correlation between TLR4 expression levels and MAPK/ERK signaling activation. Consistently, chemical blockade of MAPK/ERK signaling abrogated $BRAF^{V600E}$-induced TLR4 expression. A detailed study of the TLR4 promoter revealed a critical MAPK/ERK-sensitive Ets binding-site involved in $BRAF^{V600E}$ responsiveness. Subsequent investigation revealed that the Ets-binding factor ETS1 is critical for $BRAF^{V600E}$-induced MAPK/ERK signaling-dependent TLR4 gene expression. Together, these data indicate that functional TLR4 overexpression in PTCs is a consequence of thyroid tumor-oncogenic driver dysregulation of MAPK/ERK/ETS1 signaling.

IMPLICATIONS: Considering the participation of aberrant NF-κB signaling activation in the promotion of thyroid tumor growth and the association of high TLR4 expression with more aggressive tumors, this study suggests a pro-oncogenic potential of TLR4 downstream signaling in thyroid tumorigenesis.

KEYWORDS: Papillary thyroid carcinoma, $BRAF^{V600E}$, Toll-like receptor 4, MAPK/ERK signaling pathway, ETS-domain transcription factor family.

INTRODUCTION

The emerging role of Toll-like receptors (TLRs) in the maintenance of tissue homeostasis as critical regulators of inflammatory processes and tissue regeneration response under physiological conditions has led to the identification of aberrant functions of these receptors in different diseases, including inflammatory and infectious disorders, autoimmunity and cancer (1). Particularly, unregulated TLR signaling has been described in several neoplastic processes associated with exacerbated production of pro-inflammatory cytokines involved in tumor progression (1,2). Indeed, TLR signaling-deficient mice are resistant to tumor development in different experimental models (3,4). Likewise, transgenic mice overexpressing constitutively active TLR4 under the intestine-specific villin promoter are highly susceptible to colitis-associated cancer (5). The close link between dysregulated TLRs function and cancer progression has set the molecular basis for the development of potential therapeutics targeting TLRs or TLRs-triggered intracellular signal pathways (6).

Chronic activation of the immune system and tissue response might generate an inadequate negative regulation of TLRs signal pathways leading to an excessive pro-inflammatory microenvironment that facilitates the promotion of neoplastic processes (7). Different TLRs polymorphisms have been associated with increased susceptibility or severity of infections (8). Of note, the polymorphism rs4986790 in TLR4 gene was identified as risk factor for the development of gastric cancer in *Helicobacter pylori*-infected patients (9).

Functional TLRs expression in tumor cells has been linked to tumor survival and progression, evasion of immune system and resistance to apoptosis. TLR4 engagement in lung cancer cells induces the expression of immunosuppressive and pro-angiogenic cytokines (10). Further studies in prostate cancer cells showed that TLR4 activation promotes the secretion of pro-angiogenic cytokines in response to NF-κB signaling (11). However, discrepancies regarding tumor cell survival in response to TLR4 activation in different cell models have been observed. Particularly, TLR4 signaling improves survival in ovarian cancer cells (12) and promotes the invasive ability of colon cancer cells (13). Conversely, studies in pituitary tumors showed that TLR4 activation inhibited tumor growth (14).

In the thyroid tissue, functional TLR3 expression was reported in normal thyrocytes. McCall *et al.* (15) demonstrated high constitutive TLR3 signaling in papillary thyroid carcinomas (PTCs) compared to normal thyroid tissue and follicular thyroid carcinomas (FTCs). Moreover, phenylmethimazole—a small molecule that decreases TLR3 expression and signaling—inhibited PTC cells growth and migration (15). In addition, we demonstrated functional TLR4 expression in normal murine thyrocytes (16). Using the exogenous TLR4-agonist lipopolysaccharide (LPS), we demonstrated that NF-κB signaling plays a central role in the regulation of TLR4-induced thyroid differentiation markers gene expression (17,18). Interestingly, Hagström *et al.* (19) reported a significant correlation between high TLR4 protein levels and metastatic potential in FTCs. Moreover, Dang *et al.* (20) demonstrated that TLR4 is abundantly expressed in PTCs and stimulation of the PTC cell line W3 with the endogenous TLR4-agonist low molecular weight hyaluronic acid promotes cell proliferation and migration.

Here, we investigated the molecular events downstream thyroid cancer-driving oncogenes involved in the upregulation of TLR4 gene expression in differentiated thyroid carcinomas. As previously described, we show that TLR4 is aberrantly overexpressed in PTCs and FTCs. Moreover, TLR4 expression is functional as its exogenous agonist LPS increased NF-κB transcriptional activity in PTC cell models. Consistent with transcriptomic data of PTC showing a significant correlation between TLR4 mRNA expression levels and ERK activation score, chemical blockage of MAPK/ERK signaling abrogated $BRAF^{V600E}$-induced TLR4 expression.

MAPK/ERK signaling-dependent $BRAF^{V600E}$-induced TLR4 gene expression relies on a distal Ets binding-site identified in the TLR4 promoter. Moreover, we show that the Ets-binding factor ETS1 is critical for $BRAF^{V600E}$-induced MAPK/ERK signaling-mediated TLR4 gene expression in thyroid carcinomas. In sum, high TLR4 levels in PTC cells is the consequence of dysregulated MAPK/ERK signaling as result of thyroid tumors-drivers such as $BRAF^{V600E}$. Altogether, our evidence suggests a pro-oncogenic potential of TLR4 signaling in thyroid tumorigenesis, further considering the oncogenic potential of NF-κB signaling in the promotion of thyroid cancer (21).

MATERIAL AND METHODS

Immunohistochemistry. TLR4 and ETS1 expression in clinical thyroid samples was studied using low and high-density human thyroid tissue arrays (US Biomax - Rockville, MD, USA). Endogenous peroxidase activity was blocked by treatment with H_2O_2 in methanol for 15 min. Thyroid sections were then incubated for 30 min in 5% normal rabbit serum to block non-specific binding, followed by overnight incubation with 1 µg/ml goat polyclonal anti-TLR4 antibody (sc-16240, Santa Cruz Biotechnology - Santa Cruz, CA, USA), 5 µg/ml mouse monoclonal anti-TLR4 antibody (ab-22048, Abcam - Cambridge, MA, USA) or 3.3 µg/ml rabbit polyclonal anti-ETS1 antibody (sc-350, Santa Cruz Biotechnology) at 4 °C in a humidified chamber. For negative controls, the primary antibody was replaced by the corresponding purified non-reactive IgG in a separate slide containing paraffin-embedded thyroid carcinoma tissue samples. Afterward, thyroid sections were incubated with biotinylated secondary antibody (Santa Cruz Biotechnology) and ABC complex (Vector Laboratories - Burlingame, CA, USA). 3,3'-Diaminobenzidine (DAB) (Sigma-Aldrich, St Louis, MO, USA) was used as the chromogenic substrate for 10 min at RT, and the sections were rinsed in running water and counterstained with Harris hematoxylin. Digital images were captured at 400x magnification using a Nikon Eclipse TE2000-U light microscope (Nikon Instruments, Japan). Quantification of TLR4 and ETS-1 protein levels was performed by assessing DAB staining intensity relative to the number of cells in the histological sections in order to correct differences in tissue architecture. DAB staining intensity and the number of nuclei seen in one randomly selected area of each tissue section were quantified using ImageJ software (National Institute of Health - Bethesda, MD, USA).

Plasmids. The expression vectors encoding human $BRAF^{V600E}$ and dominant-negative human Δ152–296 MyD88 were as reported (22,23). pCMV-mFlagEts1 (plasmid #86099) was from Addgene (Cambridge, MA, USA). The NF-κB reporter vector containing five κB consensus sites linked to the luciferase coding sequence (5x κB-Luc) and the expression vector encoding dominant-negative mouse Δ670-835 TLR4 were from Clontech (Palo Alto, CA, USA) and InvivoGen (San Diego, CA, USA), respectively. Mouse TLR4 promoter constructs +52/+223, -104/+223, -336/+223 and -608/+223 were as reported (24). Disruption of the distal Ets binding-site in the mouse TLR4 promoter was performed by PCR with the oligonucleotide 5'-TGGGTTTTAATCTCTAGCATTGTGAGAAAATATGTAGTTCTAGTCTGAAACATCCA carrying the desire mutation (underlined) using KOD Hot Start DNA polymerase (EMD Millipore - Temecula, CA, USA) as described (25). The artificial ETS reporter 3x Ets^d-Luc contains the luciferase gene under the control of a promoter containing three copies in tandem of the flanking region of the distal Ets binding-site (AAAATATGTTCCTCTAGTCTGA) of mouse TLR4 promoter upstream the adenovirus E1B core promoter. The normalization reporter pCMV-β-galactosidase was obtained from Promega (Madison, WI, USA). All constructs were sequenced to verify nucleotide sequence (Instituto Nacional de Tecnología Agropecuaria, Buenos Aires, Argentina).

Cell culture. The Fischer rat thyroid cell line PCCl3 was kindly provided by Dr. Roberto Di Lauro (Università degli Studi di Napoli Federico II, Naples, Italy). PCCl3 thyroid cells engineered to obtain doxycycline-inducible expression of the oncogenes $BRAF^{V600E}$ (PC/$BRAF^{V600E}$), RET/PTC3 (PC/PTC3) and $HRas^{G12V}$ (PC/$HRas^{G12V}$) were generously provided by Dr. James Fagin (Memorial Sloan-Kettering Cancer Center, New York, USA). PCCl3 and PCCl3-derived cells were cultured in DMEM/Ham F-12 medium supplemented with 5% calf serum (Thermo-Fisher Scientific - Waltham, MA, USA), 1 mIU/ml bovine TSH (National Hormone and Peptide Program, Harbor-UCLA Medical Center - Torrance, CA, USA), 10 µg/ml bovine insulin and 5 µg/ml bovine transferrin (Sigma-Aldrich) and treated with 1 µg/ml of doxycycline (Sigma-Aldrich) to induce oncogene expression (26). Non-tumoral human thyroid cell line Nthy-ori 3-1 was obtained from the

European Collection of Authenticated Cell Cultures (Salisbury, United Kingdom) and human PTC-derived cell line BCPAP—harboring the $BRAF^{V600E}$ mutation—was provided by Dr. Massimo Santoro (Università degli Studi di Napoli Federico II, Naples, Italy). Human thyroid cells were cultured in DMEM medium supplemented with 10% fetal bovine serum (PAA Laboratories, Pasching, Austria). Human cell lines were authenticated using short tandem repeat genotyping using PowerPlex Fusion System (Promega) at Centro de Excelencia en Procesos y Productos de Córdoba (Córdoba, Argentina). Cells were also regularly tested for mycoplasma contamination using in-house PCR assays. Chemical inhibitors were obtained from the following suppliers and used at the indicated concentrations: PLX4032 (Selleck Chemicals - Houston, TX, USA), BAY 11-7082 (Sigma-Aldrich) and U0126 (Cell Signaling Technology - Danvers, MA, USA). The endotoxin lipopolysaccharide from E. coli 055:B5 was purchased from Sigma-Aldrich.

Transgenic Mice. FVB/N mice carrying thyroid-specific human $BRAF^{V600E}$ gene expression under the regulation of the bovine thyroglobulin promoter (Tg-$BRAF^{V600E}$) were provided by Dr. James Fagin (27). All procedures were approved by the Institute of Biomedical Sciences, University of São Paulo (São Paulo, Brazil) Ethical Committee for Animal Research.

RNA isolation and Real-time PCR. Total RNA purification, cDNA synthesis, and quantitative PCR (qPCR) were performed as described (28). Gene specific primer sets were as follow: mouse/rat TLR4 (180 bp) 5'-CCAAGAACCTRGAYCTGAGC (forward) and 5'-TCTTGATAGGGTTTCCTGTC (reverse), human TLR4 (180 bp) 5'-CCAAGAACCTGGACCTGAGC (forward) and 5'-TCTGGATGGGGTTTCCTGTC (reverse), rat IL-6 (109 bp) 5'-GACAAAGCCAGAGTCATTCAGAGC (forward) and 5'-GAGCATTGGAAGTTGGGGTAGG (reverse), rat iNOS (137 bp) 5'-CTTCCGAAGTTTCTGGCAGCAG (forward) and 5'-GGACCATCTCCTGCATTTCTTCC (reverse), human IL-6 (290 bp) 5'-GGATGCTTCCAATCTGGATTCAATGAG (forward) and 5'-CGCAGAATGAGATGAGTTGTCATGTCC (reverse), human iNOS (104 bp) 5'- TGGCAGCATCAGAGGGGACC (forward) and 5'-GCAGGACAGGGGACCACATCGAA (reverse), human β-actin (109 bp) 5'-ACTCTTCCAGCCTTCCTTCC (forward) and 5'- GTTGGCGTACAGGTCTTTGC (reverse), rat β-actin (223 bp) 5'- CTACAATGAGCTGCGTGTGG (forward) and 5'- GGGCACAGTGTGGGTGAC (reverse), mouse β-actin (157 bp) 5'- CAGCTTCTTTGCAGCTCCTT (forward) and 5'- CACGATGGAGGGGAATACAG (reverse). Relative changes in gene expression were calculated using the $2^{-\Delta\Delta Ct}$ method normalized against the housekeeping gene β-actin. For each pair of primers a dissociation plot resulted in a single peak, indicating that only one cDNA species was amplified. The amplification efficiency for each pair of primers was calculated using standard curves generated by serial dilutions of cDNA generated from PCCl3 or BCPAP cells. All amplification efficiencies ranged between 97-105% in different assays.

Immunoblotting. SDS-PAGE, electrotransference to nitrocellulose membranes, and immunoblotting were as described (29). Membranes were incubated with 0.2 µg/ml mouse monoclonal anti-TLR4 (ab-22048, Abcam), 0.2 µg/ml rabbit polyclonal anti-BRAF (sc-166, Santa Cruz Biotechnology), 0.2 µg/ml mouse monoclonal anti-p-ERK (sc-7383, Santa Cruz Biotechnology), 0.2 µg/ml rabbit polyclonal anti-ERK (sc-94, Santa Cruz Biotechnology), 0.2 µg/ml rabbit polyclonal anti-ETS1 (sc-350, Santa Cruz Biotechnology), 0.2 µg/ml rabbit polyclonal anti-PARP-1 (sc-7150, Santa Cruz Biotechnology), 0.4 µg/ml mouse monoclonal anti-α-Tubulin (T6074, Sigma-Aldrich) antibodies. After washing, membranes were further incubated with IRDye 680 RD or IRDye 800 CW-linked secondary anti-rabbit and anti-mouse antibodies (LI-COR Biotechnology - Lincoln, NE, USA), protected from light. Membranes were visualized and quantified by Odyssey Infrared Imaging System (LI-COR Biotechnology). Equal loading was assessed by stripping and reprobing the same blot with 0.1 µg/ml rabbit polyclonal anti-GAPDH (sc-25778, Santa Cruz Biotechnology).

Immunofluorescence. Cells seeded onto glass coverslips were fixed in 2% paraformaldehyde (30). Cells were immunostained with 10 µg/ml mouse monoclonal anti-TLR4 (ab-22048, Abcam) or 4 µg/ml rabbit polyclonal anti-ETS1 (sc-350, Santa Cruz Biotechnology) in PBS containing 0.2% BSA. For analysis under permeabilized conditions an additional 0.1% Triton was added. Secondary staining proceeded with 50 nM anti-mouse Alexa-594 antibody (Thermo-Fisher Scientific). Nuclear DNA was stained with 4',6-diamidino-2-phenylindole (DAPI). Coverslips were mounted with FluorSave Reagent (EMD Millipore) and images were acquired on a Leica DMi8 epifluorescence microscope (Leica Microsystems - Buffalo Grove, IL, USA). The number of nuclei and the intensity of TLR4 or ETS1 immunostaining were analyzed using ImageJ software.

Transient transfection and reporter gene assay. Cells were transiently co-transfected with 0.64 µg/well of luciferase reporter vectors or 0.21 µg/well of luciferase reporter vectors plus 0.42 µg/well of expression vectors and 0.16 µg/well of the normalization reporter β-galactosidase in 24-well plates using Lipofectamine 2000 (Thermo-Fisher Scientific) (29). The luciferase activity was measured using a Luciferase Assay System (Promega) according to the manufacturer's instructions and normalized relative to that of β-galactosidase.

Small interference RNA. Negative control siRNA pool (D-001206-13) and rat siRNA specific for ETS1 (sc-156062) were from Dharmacon (Lafayette, CO, USA) and Santa Cruz Biotechnology, respectively. PC/BRAF^{V600E} cells were seeded at a density of 5x10^5 cells/well onto 6-well plates and transfected with 10 nM of each siRNA pool using Lipofectamine RNAiMAX reagent (Thermo-Fisher Scientific) according to the manufacturer's protocol. ETS1 protein expression was monitored by immunoblotting 48 h after transfection.

Chromatin Immunoprecipitation (ChIP). Cells were crosslinked in culture media containing 1% formaldehyde and nuclei were purified and lysed in 50 mM Tris-HCl (pH 8), 10 mM EDTA and 1% sodium dodecyl sulfate (31). Genomic DNA was broken by sonication and 10-fold diluted in IP Dilution Buffer [50 mM Tris-HCl (pH 7.5), 150 mM NaCl, 5 mM EDTA, 1% Triton X-100 and 0.5% Nonidet P-40]. Immunoprecipitation was performed with 2 µg non-specific mouse IgG or rabbit polyclonal anti-ETS1 antibody (sc-350, Santa Cruz Biotechnology) (32). Immune complexes were purified with Protein A/G PLUS-Agarose (Santa Cruz Biotechnology) pre-blocked with sonicated salmon sperm DNA (Sigma-Aldrich). Immunoprecipitates were washed four times with IP Dilution Buffer containing 0.1% SDS; twice with High Salt IP Wash Buffer [50 mM Tris-HCl (pH 7.5), 500 mM NaCl, 5 mM EDTA, 0.1% SDS and 1% Triton X-100], and once with TE [10 mM Tris-HCl (pH 8), 1 mM EDTA]. DNA was purified using Chelex-100 (Bio-Rad – Hercules, CA, USA). Immunoprecipitated DNA was quantified by qPCR using the primer set 5'-GAGAGAGGTCTATTGCCCCATG (forward) and 5'-AGCGTTTGCTGACCAGCTTC (reverse) as described. Relative fold of increase were calculated according to the equation: $2^{-[(Ct.input - Ct.target) – (Ct.input - Ct.mock)]}$.

Statistical analysis. Results are reported as the mean ± SEM from at least three independent experiments. Multiple group analysis was conducted by one-way ANOVA with Newman-Keuls multiple comparisons post-test. Comparisons between two groups were performed using unpaired Student's t test or nonparametric Mann-Whitney test. Immunohistochemistry quantifications were analyzed by the nonparametric Kruskal-Wallis test with Dunn's multiple comparison post hoc tests. Correlation and disease-free survival analysis using molecular data derived from The Cancer Genome Atlas were analyzed using Spearman's correlation coefficient and Mantel-Cox test, respectively. Statistical analyses were performed using GraphPad Prism (GraphPad Software - La Jolla, CA, USA). Differences were considered statistically significant at $P < 0.05$.

RESULTS

TLR4 is overexpressed in differentiated thyroid carcinomas. We studied TLR4 expression in normal (n=13) and malignant thyroid sections, including PTC (n=50) and FTC (n=32) by immunohistochemistry. In agreement with previous observations (16,19,20), TLR4 expression was detected on normal thyrocytes (Fig. 1A). Interestingly, TLR4 protein levels were significantly higher in differentiated—follicular and papillary—thyroid carcinomas compared to normal thyroid tissue (Fig. 1A), although no statistical differences were evidenced between papillary and follicular thyroid tumors (Fig. 1A). Moreover, similar changes in TLR4 protein expression were evidenced in independent assays using a different anti-TLR4 antibody (Fig. S1). Of note, comparison of TLR4 expression levels between matched-samples of tumor adjacent normal thyroid tissue and PTCs (n=4) showed a significant upregulation of TLR4 levels in the neoplastic tissue (Fig. 1B). No significant correlation was evidenced between TLR4 protein immunostaining and tumor, node and metastasis (TNM) staging in PTCs or FTCs (Fig. S2). Significantly, TLR4 protein expression was also detected in lymph node metastasis derived from PTCs (Fig. 1C). Comparison of TLR4 expression levels between matched-samples of primary PTCs and its lymph node metastasis (n=8) showed a significant upregulation of TLR4 levels in the metastatic tissue (Fig. 1C).

Thereafter, we used molecular data derived from The Cancer Genome Atlas (TCGA) study of PTC (33) to perform combined analysis of TLR4 mRNA expression as a function of the most frequent driver oncogenes identified in PTCs, including point mutations and gene fusions (33). Although TLR4 mRNA levels were found unaltered in PTCs harboring different tumor driving oncogenes, we noticed a highly heterogeneous TLR4 expression among PTCs harboring the same oncogene (Fig. 1D). However, a significant positive correlation was evidenced between TLR4 mRNA expression levels and ERK activation score (r_s=0.1280, *P*=0.0189), an evaluation of the activation status of MAPK/ERK signaling (33), suggesting that oncogene-stimulated MAPK/ERK signaling is an important event driving TLR4 gene expression in PTCs (Fig. 1E). In agreement, the Gene Expression Omnibus (GEO) dataset GSE33630 analysis also showed a significant positive correlation between TLR4 mRNA expression levels and ERK activation score in PTC (Fig. S3).

Thereafter, we focused our analysis on PTCs harboring the oncogene $BRAF^{V600E}$ as this mutation has been reported to occur in 30-80% of PTCs (34). We evidenced a significant positive correlation between TLR4 mRNA expression and the thyroid differentiation score (r_s=0.1436, *P*=0.0302), an evaluation of the dedifferentiation status of the tumor (33), supporting that TLR4 gene expression is higher in more differentiated PTCs (Fig. 1F). Moreover, we observed a non-significant positive association between TLR4 mRNA expression and MACIS score (r_s=0.1039, *P*=0.1548), an outcome predictor in patients with PTC (Fig. 1G). The modest association may be due in part to the characteristics of the patients, as most of them fall into the low-risk category (MACIS score <6). Thereafter, patient samples harboring the oncogene $BRAF^{V600E}$ (wild-type TERT status) were divided into the high or low cohort based on the median expression of TLR4 mRNA levels within the group. Interestingly, patients whose tumors showed high TLR4 expression, based on TLR4 expression above the median, had a lower median disease-free survival than those who showed TLR4 expression below the median ($TLR4^{high}$=26.63 months vs. $TLR4^{low}$=31.24 months, *P*=0.0071) (Fig. 1H). Together, these data suggest that TLR4 mRNA expression constitutes a potential marker of PTC aggressiveness.

PTC-driving oncogenes induce TLR4 expression. In order to study oncogene-driving TLR4 gene expression, we analyzed TLR4 mRNA expression in PCCl3 thyroid cell conditionally expressing the oncogenes $BRAF^{V600E}$, $HRAS^{G12V}$, or RET/PTC3 in response to doxycycline. In PCCl3 cells, doxycycline treatment did not up-regulate

TLR4 mRNA expression. Conversely, in PC/BRAF^{V600E}, PC/HRas^{G12V} and PC/PTC3 cells doxycycline-induced oncogene expression was associated with a significant increase of TLR4 mRNA expression (Fig. 2A). Additionally, we assessed TLR4 protein expression in PC/BRAF^{V600E} cells in response to doxycycline. BRAF^{V600E} expression significantly increased TLR4 protein levels in PC/BRAF^{V600E} cells (Fig. 2B). Furthermore, transient transfection of BRAF^{V600E} into non-tumoral Nthy-ori 3-1 thyroid cells significantly increased TLR4 protein expression levels compared to those of empty vector-transfected cells (Fig. 2C). Analysis of ERK phosphorylation was used to assess BRAF^{V600E} oncogenic activity. Complementary, immunofluorescence performed under non-permeabilized conditions showed increased TLR4 protein levels at the plasma membrane in response to BRAF^{V600E} expression (Fig. 2D). Similar observations were done in PCCl3 cells conditionally expressing the oncogenes HRas^{G12V} and RET/PTC3 (Fig. S4).

In order to further confirm our findings, TLR4 mRNA expression was studied in five-week old transgenic mice conditionally expressing the oncogene BRAF^{V600E} in the thyroid follicular cell (27). The thyroid tumors of transgenic mice showed significantly higher TLR4 mRNA expression levels compared to that of non-transgenic littermates controls (Fig. 2E). In addition, the expression of TLR4 protein levels in paraffin-embedded normal and malignant mice thyroid tissues was assessed by immunohistochemistry. Accordingly, TLR4 immunostaining was significantly increased in the thyroid tumor tissue of BRAF^{V600E}-expresing mice compared to littermates controls (Fig. 2F).

Functional TLR4 protein expression in cell models of PTC. All TLRs signaling pathways culminate in activation of the transcription factor NF-κB (35). Therefore, the functionality of TLR4 overexpression in thyroid carcinomas was assessed by analyzing NF-κB signaling activation in response to the TLR4 agonist LPS. Consistently with previous observations indicating the activation of NF-κB signaling in response to BRAF^{V600E} expression (34), doxycycline-treated PC/BRAF^{V600E} cells showed a significant induction of the NF-κB reporter 5x κB-Luc (Fig. 3A). Interestingly, LPS treatment induced a significant upregulation of NF-κB transcriptional activity in doxycycline-treated PC/BRAF^{V600E} cells (Fig. 3A). The NF-κB inhibitor BAY 11-7082 was used to investigate the specific activation of NF-κB pathway (Fig. 3A). Moreover, consistently with the activation of NF-κB signaling in response to TLR4 activation, we observed a significant BAY 11-7082-sensitive increase in the mRNA expression of the well-known TLR4-induced NF-κB targets interleukin-6 (IL-6) and inducible nitric oxide synthase (iNOS) in response to LPS stimulation in doxycycline-treated PC/BRAF^{V600E} cells (Fig. 3B and C).

In order to reinforce our observations, we further studied the activation of NF-κB signaling in response to the TLR4-agonist LPS in BCPAP cells harboring the BRAF^{V600E} mutation. LPS stimulation of NF-κB reporter-transiently transfected BCPAP cells showed a significant induction of NF-κB transcriptional activity (Fig. 3D). As mentioned, assay specificity was verified by inhibiting the activation of NF-κB signaling using BAY 11-7082 (Fig. 3D). Additionally, we evidenced that BCPAP cells transiently expressing a non-signaling TLR4 mutant missing the carboxy-terminus or a non-signaling MyD88—intracellular TLR4 signaling adaptor—mutant missing the TLR4-interacting domain were not responsive to LPS stimulation (Fig. 3D). Consistently, LPS-induced TLR4-dependent signaling increased IL-6 and iNOS mRNA expression in BCPAP cells (Fig. 3E and F). Together, this evidence suggests that TLR4/MyD88/NF-κB signaling is functionally conserved in the PTC cell line BCPAP.

BRAF^{V600E}-induced TLR4 gene expression involves MEK/ERK signal pathway. The oncogene BRAF^{V600E} leads to constitutive activation of MAPK/ERK pathway by directly phosphorylating MEK, resulting in thyroid follicular cell transformation (23,34). To uncover the signal pathway involved in the regulation of TLR4 gene expression in response to BRAF^{V600E} activity, we explored the effect of the specific BRAF^{V600E} inhibitor PLX4032 and the MEK1/2 inhibitor U0126 on TLR4 expression in PC/BRAF^{V600E} cells under doxycycline treatment. As expected, BRAF^{V600E} inhibition reduced the upregulated TLR4 expression in response to doxycycline treatment (Fig. 4A). In line with the observed positive correlation between TLR4 expression and MAPK/ERK activation score, chemical inhibition of MAPK/ERK signaling activation reduced TLR4 expression in response to BRAF^{V600E} induction (Fig. 4A). We analyzed ERK phosphorylation status by immunoblot to assess the inhibition of BRAF^{V600E}-induced MAPK/ERK signaling in response to PLX4032 or U0126 treatment (Fig. 4A). Complementary, immunofluorescence performed under non-permeabilized conditions showed that chemical inhibition of MAPK/ERK signaling abrogated BRAF^{V600E}-induced cell surface TLR4 protein expression levels (Fig. S5). Moreover, chemical inhibition of MAPK/ERK signaling activation reduced TLR4 mRNA expression in response to BRAF^{V600E} induction (Fig. 4B). To confirm this finding, we studied BRAF^{V600E}-regulated TLR4 gene expression in BCPAP cells. Interestingly, BCPAP cells treated with the chemical inhibitors PLX4032 or U0126 showed a significant reduction of TLR4 protein and mRNA expression levels (Fig. 4C and D). Altogether, these observations reinforce the involvement of MAPK/ERK signaling in the BRAF^{V600E}-regulated TLR4 gene expression.

A distal E26 transformation-specific (Ets)-binding site is crucial for TLR4 gene transcription in response to constitutive BRAF^{V600E} signaling. To uncover the molecular mechanism involved in the BRAF^{V600E}-induced TLR4 gene expression, we studied the transcriptional activity of sequential mouse TLR4 promoter deletions linked to luciferase in doxycycline-treated PC/BRAF^{V600E} cells. The TLR4 promoter constructs -336/+223 and -608/+223 showed a significant transcriptional response to the induction of BRAF^{V600E} expression (Fig. 5A). However, the promoter constructs +52/+223 and -104/+223 abrogated BRAF^{V600E}-induced TLR4 transcriptional activity (Fig. 5A). As reported, the sequence of the TLR4 promoter comprising nucleotides -336 and -104 contains a distal Ets-binding site (Ets^{d}) critical for constitutive TLR4 expression in mouse macrophages (24). Thereafter, we performed site-directed mutagenesis of the Ets^{d} DNA-binding site within the −336/+223 promoter construct. Significantly, Ets^{d} mutagenesis reduced BRAF^{V600E}-induced TLR4 promoter activity (Fig. 5B). Similar observations were done in PCCl3 cells conditionally expressing the oncogenes HRas^{G12V} and RET/PTC3 (Fig. S6).

In order to further test our observations, we constructed an artificial reporter containing three copies in tandem of the flanking region of the Ets^{d} binding site linked to luciferase (3x Ets^{d}-Luc). Significantly, BRAF^{V600E} expression increased the luciferase activity of PC/BRAF^{V600E} cells transiently transfected with the trimeric Ets^{d} reporter construct (Fig. 5C). Moreover, we observed that the transcriptional activity of the −336/+223 TLR4 promoter construct missing the Ets^{d} binding site (Ets^{d} mt -336/+223) was significantly lower than that of the wild type promoter in BCPAP thyroid cancer cells (Fig. 5D). Together, these results support the involvement of the distal Ets-binding site in the transcriptional upregulation of TLR4 in response to BRAF^{V600E} expression.

The Ets-binding protein ETS1 mediates BRAF^{V600E}-induced TLR4 gene expression. Ets-binding proteins (ETSs) are a family of transcription factors that share a conserved ~85 amino-acid sequence called Ets DNA-binding domain (36). ETS transcription factors are involved in a wide variety of functions including

differentiation, proliferation, migration, apoptosis and angiogenesis. Significantly RAS/RAF signaling increases the transcriptional activity of some, but not all, ETS transcription factors through direct phosphorylation of MAPK/ERK signaling (36).

To uncover the downstream $BRAF^{V600E}$-induced ETS factors required for TLR4 gene overexpression, we used transcriptomic data derived from TCGA of PTC (33) to correlate the mRNA expression of TLR4 and different members of the ETS family in the subset of PTCs harboring the oncogene $BRAF^{V600E}$. Interestingly, although a significant positive correlation with ELF1, ETV3 and GABPA, and negative correlation with ETV4 and ELK1 were evidenced (Fig. S7A), the ETS ETS1 showed the highest positive association with TLR4 mRNA levels ($r=0.5788$, $P<0.0001$) (Fig. 6A), suggesting a potential role for ETS1 in the $BRAF^{V600E}$-induced TLR4 gene overexpression in PTCs. In agreement, GEO dataset GSE33630 analysis also showed that the ETS family member ETS1 has the highest positive correlation with TLR4 mRNA expression in PTCs (Fig. S7B). Supporting these findings, ETS1 mRNA expression is up-regulated in PTCs harboring the oncogene $BRAF^{V600E}$ (37) and constitutes a critical genome-wide transcriptional effector of RAS/ERK signaling in tumor epithelial cells (32).

We further explored ETS1 protein expression in tissue microarrays containing unmatched normal thyroid tissue (n=9) and PTCs (n=24) by immunohistochemistry. Although in the normal thyroid tissue ETS1 protein expression was detected at low levels, its expression was significantly upregulated in PTC (Fig. 6B). In tumor tissues, assessment of high-magnification images suggested that ETS1 was localized in both the cytoplasm and nucleus. Moreover, correlation analysis demonstrated a significant positive correlation between TLR4 and ETS1 protein levels reinforcing a potential involvement of ETS1 transcriptional activity in TLR4 expression levels (Fig. 6C).

To elucidate the involvement of ETS1 as downstream target of $BRAF^{V600E}$ oncogenic activity, we studied ETS1 protein expression in response to doxycycline treatment in PC/$BRAF^{V600E}$ cells. Conditional $BRAF^{V600E}$ expression promoted an increase of ETS1 protein expression and its nuclear accumulation (Fig. 6D and E). In addition, we evidenced the involvement of MAPK/ERK signaling in the $BRAF^{V600E}$-dependent ETS1 protein expression in PC/$BRAF^{V600E}$ and BCPAP cells (Fig. 6F and G).

Moreover, in order to analyze the involvement of ETS1 in TLR4 gene expression, we studied $BRAF^{V600E}$-induced TLR4 mRNA expression in ETS1 knock-down PC/$BRAF^{V600E}$cells. Immunoblot analysis showed a successful knock-down of ETS1 protein levels in ETS1 siRNA transfected cells compared to scrambled (SCR) siRNA-transfected cells (Fig. 6H). Interestingly, we evidenced a significant inhibition of $BRAF^{V600E}$-induced TLR4 mRNA expression levels in ETS1 knock-down cells compared to those of SCR siRNA-transfected cells (Fig. 6I). Consistently, analysis of TLR4 promoter activity showed that ETS1 knock-down repressed the $BRAF^{V600E}$-increased TLR4 transcriptional activity (Fig. 6J). In agreement, TLR4 protein expression (Fig. 6K) and its promoter activity (Fig. 6L) showed a significant upregulation in PCCl3 normal thyroid cells transiently transfected to achieve ETS1 overexpression.

Thereafter, we studied ETS1 binding to the TLR4 promoter in response to $BRAF^{V600E}$ expression in PC/$BRAF^{V600E}$ cells using ChIP assays. In detail, one putative Ets-binding site located between -240 and -233 (relative to the transcription start site) in the rat TLR4 promoter was evidenced when its sequence was analyzed for putative Ets-binding sites using MatInspector software (Genomatix AG, Munich, Germany). Interestingly, ChIP assay with an anti-ETS1 antibody of doxycycline-treated PC/$BRAF^{V600E}$ cells revealed a significant enrichment in the TLR4 promoter sequence flanking the Ets-binding site (Fig. 6M). These data indicated that $BRAF^{V600E}$-induced activation of MAPK/ERK signaling up-regulated directly ETS1 expression and binding to the TLR4 promoter that, in turn, modulated TLR4 gene expression.

DISCUSSION

Accumulating evidence indicates the association between over-activation of TLRs signaling and cancer progression (1). Indeed, dysregulated TLRs signaling has been reported in several human cancers and related to an exacerbated production of a pro-inflammatory tumor microenvironment that provides the necessary context for tumor progression, angiogenesis, invasion, metastasis and evasion of immune surveillance (2). The biological relevance of TLRs expression in tumor cells seems complex, and the regulatory mechanisms leading to differential TLRs expression in cancer cells remains unclear.

In the thyroid tissue, we demonstrated functional TLR4 expression in normal murine thyrocytes as TLR4 engagement increased the expression of differentiation markers involved in thyroid hormonogenesis (16-18). Here, in agreement with previous studies (19,20), we evidenced the presence of TLR4 protein overexpression in well-differentiated thyroid carcinoma compared to that of normal thyroid tissue. Moreover, we observed a significant up-regulation of TLR4 protein levels in lymph node metastasis derived from PTCs. Unfortunately, a limitation of our immunohistochemical study of thyroid tumor sections is the unavailability of information regarding the oncogenic driver promoting thyroid tumorigenesis. Therefore, we were unable to assess whether upregulated TLR4 protein expression is restricted to a particular oncogenic context. However, we did not evidence different TLR4 mRNA expression patterns among PTCs harboring different tumor driving oncogenes. Additionally, integrative analysis of clinical and transcriptomic data derived from TCGA of PTC (33) demonstrated that patients whose $BRAF^{V600E}$-positive tumor showed high TLR4 expression, based on TLR4 expression above the median, had a lower median disease-free survival than those who showed TLR4 expression below the median. In close correlation, Dang *et al.* (20) demonstrated a higher incidence of lymph node and distant metastasis in patients with PTC showing high TLR4 expression levels. Mechanistically, these authors demonstrated that TLR4 engagement with low molecular weight hyaluronic acid induced a significant upregulation of CXCR7, the receptor of the chemokine CXCL12 involved in the promotion of tumor cell proliferation and migration (20). Although these findings support a potential pro-metastatic role for TLR4-mediated signaling in thyroid tumorigenesis, its participation in PTC aggressiveness and metastatic potential should be further evaluated.

The ETSs regulate a plethora of processes, including differentiation, proliferation, apoptosis, and angiogenesis downstream MAPK/ERK signaling activation (36). Significantly, aberrant ETSs activation has been reported in several solid tumors (36). Particularly, the transcriptional activity of ETS1 and ETS2 is required for thyroid follicular cell transformation (38). Here, we provided novel evidence regarding the mechanisms that result in functional TLR4 overexpression in PTCs. Our data indicate that TLR4 gene overexpression in PTC is the consequence of dysregulated MAPK/ERK signaling due to thyroid cancer-driver oncogenes such as $BRAF^{V600E}$. Roger *et al.* (24) carried out a detailed study of the mechanism controlling TLR4 gene expression regulation in mouse macrophages evidencing a distal Ets-binding site indispensable for constitutive TLR4 gene transcription which may be recognized by epithelium-specific ESE1 transcription factor. In this study, we demonstrated that the same Ets-binding site in the TLR4 promoter is critical for its transcriptional up-regulation in response to $BRAF^{V600E}$ oncogenic activity. Moreover, conducting bioinformatics analysis, and biochemical approaches, we revealed the direct role of ETS1 as transcriptional regulator of TLR4 gene expression downstream to $BRAF^{V600E}$-induced MAPK-ERK signaling. In agreement, a comprehensive gene expression analysis of ETS1-regulated genes in PC3 prostate cancer cells demonstrated that ETS1 knock-down decreases TLR4 mRNA expression, suggesting that ETS1 constitutes a positive regulator of TLR4 gene expression in cancer cells (39).

Several studies indicate that single nucleotide polymorphisms in TLRs are associated with immune system dysregulated and cancer development (8). Polymorphisms in TLRs genes may shift the balance between pro- and anti-inflammatory cytokines, modulating the risk of infection, chronic inflammation, and cancer (8). Although TLR4 has been described as a highly polymorphic gene, certain TLR4 polymorphisms have been associated with a significant risk to develop epithelial cell-derived neoplasia. Particularly, the polymorphisms rs10116253 and rs1927911 in TLR4 gene were associated with decreased risk to develop gastric cancer (40), while the polymorphisms rs4986790, rs4986791 and rs10759932 appear to be positively associated with the development of gastric cancer (41). Moreover, the polymorphism rs11536889 located in the 3'-untranslated region of the TLR4 was associated with increased prostate and colon cancer risk (42,43). In thyroid carcinomas, however, the presence of TLR4 polymorphisms remains to be investigated. Significantly, Kim *et al.* (44) reported a case-control association study of the polymorphisms rs3804099 and rs3804100 in TLR2 gene in patients with PTC and control subjects, describing a significant association between polymorphisms in the TLR2 gene and bilateral thyroid tumors, a surgical criteria to perform total thyroidectomy. More recently, Kim *et al.* (45) reported a significant association of the missense polymorphism rs11466653 in TLR10 with a higher risk for the development of thyroid papillary microcarcinomas than in the control group. Together, these findings support that abnormal TLR signaling in PTC may be involved in the interplay between inflammation and tumorigenesis.

TLRs recognize molecules that are broadly shared by pathogens but, sometimes, indistinguishable from host proteins released by stressed cells undergoing necrosis or proteolytic products derived from structural components of the extracellular matrix, collectively referred to as damage-associated molecular patterns (DAMPs). Here, we demonstrated that malignant thyroid follicular cells themselves are responsive to exogenous TLR4 agonists. However, the question regarding the endogenous molecules that engage TLR4 in the tumor environment to induce a signaling cascade leading to the NF-κB activation remains unanswered. We hypothesized that TLR4 signaling-activating DAMPs such as High mobility group box-1 (HMGB1) which is usually observed at high levels in the tumor microenvironment or hyaluronan-derived proteolytic products considering that hyaluronan is highly expressed in the tumor stroma of differentiated thyroid carcinomas (46) are likely candidates. Moreover, regarding the importance of DAMPs in thyroid tumor progression, recent evidence suggested that the multiligand receptor for advanced glycation end products (RAGE) mediates the pro-migratory response of extracellular small calcium-binding protein (S100A4) in human thyroid cancer cells (47).

TLRs-triggered signal pathways culminate in the activation of the transcription factor NF-κB, which induces the expression of pro-inflammatory cytokines, anti-apoptotic factors, and pro-angiogenic factors (35). Recent evidence indicates that NF-κB signaling, as well as the pathways that culminate in its activation, are crucial players in many steps of carcinogenesis and tumor development (48). Genetic alterations leading to constitutive MAPK/ERK signaling have a fundamental role in thyroid carcinogenesis (34). However, additional molecular derangements are associated with tumor progression and aggressiveness. Particularly, aberrant NF-κB signaling activation is triggered by different oncogenes involved in thyroid carcinogenesis associated with a papillary phenotype (49) and linked to anaplastic thyroid tumorigenesis (21). NF-κB signaling activation has been associated with tumor progression, resistance to chemotherapeutic agents-induced apoptosis and invasion associated with metalloproteinases expression (21). In close relation, the polymorphism rs2233406 in NFKBIA gene, an NF-κB signaling inhibitor, was associated with a pro-inflammatory tumor microenvironment resulting from the exacerbated TLR4-dependent secretion of IL-1β that could favor tumor progression (50).

Overall, our findings raise an intriguing question regarding the pro-oncogenic potential of TLR4 downstream signaling in thyroid tumorigenesis, further considering that dysregulated NF-κB signaling has been implicated in thyroid cancer process (21). The understanding of TLR4 function in differentiated thyroid tumor development and growth as well as the mechanisms involved in these processes could have great clinical relevance. Further uncovering the mechanisms leading to TLR4 engagement and signaling in thyroid tumors may provide novel alternatives for the establishment of future therapies for thyroid cancer, and the design of new diagnostic procedures to identify a subset of potentially aggressive PTCs.

ACKNOLEDGEMENTS

We would like to thank Dr. Di Lauro (Università degli Studi di Napoli Federico II) for kindly providing PCCl3 cells, Dr. Fagin (Memorial Sloan Kettering Cancer Center) for PCCl3 cells engineered to obtain doxycycline-inducible oncogene expression and transgenic Tg-BRAF^{V600E} mice, and Dr. Santoro (Università degli Studi di Napoli Federico II) for human thyroid cancer cell line BCPAP. Moreover, we acknowledge Dr. Calandra (Centre Hospitalier Universitaire Vaudois) and Dr. Arditi (Cedars-Sinai Medical Center) for sharing mouse TLR4 promoter constructs and dominant-negative human MyD88 expression vector, respectively. The results published here are in part based upon data generated by The Cancer Genome Atlas Research Network (http://cancergenome.nih.gov).

This work was supported by fellowships and research grants from Agencia Nacional de Promoción Científica y Tecnológica (PICT-2008-0890 and PICT-2014-2564 to A.M.M.-R. PICT-2014-0726, PICT-2015-3839 and PICT-2015-3705 to J.P.N.), Consejo Nacional de Investigaciones Científicas y Técnicas, Secretaría de Ciencia y Tecnología of Universidad Nacional de Córdoba, Latin American Thyroid Society and Thyroid Cancer Survivors' Association (to J.P.N.), Ministerio de Economía y Competitividad de España - Fondo Europeo de Desarrollo Regional (SAF2016-75531-R to P.S.) and Fundación Española contra el Cáncer (GCB14142311CRES to P.S.).

REFERENCES

1. Rakoff-Nahoum S, Medzhitov R. Toll-like receptors and cancer. Nat Rev Cancer **2009**;9:57-63.
2. Ridnour LA, Cheng RY, Switzer CH, Heinecke JL, Ambs S, Glynn S*, et al.* Molecular pathways: toll-like receptors in the tumor microenvironment--poor prognosis or new therapeutic opportunity. Clin Cancer Res **2013**;19:1340-6.
3. Fukata M, Chen A, Vamadevan AS, Cohen J, Breglio K, Krishnareddy S*, et al.* Toll-like receptor-4 promotes the development of colitis-associated colorectal tumors. Gastroenterology **2007**;133:1869-81.
4. Swann JB, Vesely MD, Silva A, Sharkey J, Akira S, Schreiber RD*, et al.* Demonstration of inflammation-induced cancer and cancer immunoediting during primary tumorigenesis. Proc Natl Acad Sci U S A **2008**;105:652-6.
5. Fukata M, Shang L, Santaolalla R, Sotolongo J, Pastorini C, Espana C*, et al.* Constitutive activation of epithelial TLR4 augments inflammatory responses to mucosal injury and drives colitis-associated tumorigenesis. Inflamm Bowel Dis **2011**;17:1464-73.
6. Pradere JP, Dapito DH, Schwabe RF. The Yin and Yang of Toll-like receptors in cancer. Oncogene **2014**;33:3485-95.
7. Grivennikov SI, Greten FR, Karin M. Immunity, inflammation, and cancer. Cell **2010**;140:833-99.
8. El-Omar EM, Ng MT, Hold GL. Polymorphisms in Toll-like receptor genes and risk of cancer. Oncogene **2008**;27:244-52.
9. Hold GL, Rabkin CS, Chow WH, Smith MG, Gammon MD, Risch HA*, et al.* A functional polymorphism of toll-like receptor 4 gene increases risk of gastric carcinoma and its precursors. Gastroenterology **2007**;132:905-12.
10. He W, Liu Q, Wang L, Chen W, Li N, Cao X. TLR4 signaling promotes immune escape of human lung cancer cells by inducing immunosuppressive cytokines and apoptosis resistance. Mol Immunol **2007**;44:2850-9.
11. Pei Z, Lin D, Song X, Li H, Yao H. TLR4 signaling promotes the expression of VEGF and TGFbeta1 in human prostate epithelial PC3 cells induced by lipopolysaccharide. Cell Immunol **2008**;254:20-7.
12. Kelly MG, Alvero AB, Chen R, Silasi DA, Abrahams VM, Chan S*, et al.* TLR-4 signaling promotes tumor growth and paclitaxel chemoresistance in ovarian cancer. Cancer Res **2006**;66:3859-68.
13. Wang JH, Manning BJ, Wu QD, Blankson S, Bouchier-Hayes D, Redmond HP. Endotoxin/lipopolysaccharide activates NF-kappa B and enhances tumor cell adhesion and invasion through a beta 1 integrin-dependent mechanism. J Immunol **2003**;170:795-804.
14. Tichomirowa M, Theodoropoulou M, Lohrer P, Schaaf L, Losa M, Uhl E*, et al.* Bacterial endotoxin (lipopolysaccharide) stimulates interleukin-6 production and inhibits growth of pituitary tumour cells expressing the toll-like receptor 4. J Neuroendocrinol **2005**;17:152-60.
15. McCall KD, Harii N, Lewis CJ, Malgor R, Kim WB, Saji M*, et al.* High basal levels of functional toll-like receptor 3 (TLR3) and noncanonical Wnt5a are expressed in papillary thyroid cancer and are coordinately decreased by phenylmethimazole together with cell proliferation and migration. Endocrinology **2007**;148:4226-37.
16. Nicola JP, Velez ML, Lucero AM, Fozzatti L, Pellizas CG, Masini-Repiso AM. Functional toll-like receptor 4 conferring lipopolysaccharide responsiveness is expressed in thyroid cells. Endocrinology **2009**;150:500-8.
17. Nazar M, Nicola JP, Velez ML, Pellizas CG, Masini-Repiso AM. Thyroid peroxidase gene expression is induced by lipopolysaccharide involving nuclear factor (NF)-kappaB p65 subunit. Endocrinology **2012**;153:6114-25.
18. Nicola JP, Nazar M, Mascanfroni ID, Pellizas CG, Masini-Repiso AM. NF-kappaB p65 subunit mediates lipopolysaccharide-induced Na(+)/I(-) symporter gene expression. Mol Endocrinol **2010**;24:1846-62.
19. Hagstrom J, Heikkila A, Siironen P, Louhimo J, Heiskanen I, Maenpaa H*, et al.* TLR-4 expression and decrease in chronic inflammation: indicators of aggressive follicular thyroid carcinoma. J Clin Pathol **2012**;65:333-8.

20. Dang S, Peng Y, Ye L, Wang Y, Qian Z, Chen Y*, et al.* Stimulation of TLR4 by LMW-HA induces metastasis in human papillary thyroid carcinoma through CXCR7. Clin Dev Immunol **2013**;2013:712561.
21. Pacifico F, Leonardi A. Role of NF-kappaB in thyroid cancer. Mol Cell Endocrinol **2010**;321:29-35.
22. Bulut Y, Faure E, Thomas L, Karahashi H, Michelsen KS, Equils O*, et al.* Chlamydial heat shock protein 60 activates macrophages and endothelial cells through Toll-like receptor 4 and MD2 in a MyD88-dependent pathway. J Immunol **2002**;168:1435-40.
23. Riesco-Eizaguirre G, Gutierrez-Martinez P, Garcia-Cabezas MA, Nistal M, Santisteban P. The oncogene BRAF V600E is associated with a high risk of recurrence and less differentiated papillary thyroid carcinoma due to the impairment of Na+/I- targeting to the membrane. Endocr Relat Cancer **2006**;13:257-69.
24. Roger T, Miconnet I, Schiesser AL, Kai H, Miyake K, Calandra T. Critical role for Ets, AP-1 and GATA-like transcription factors in regulating mouse Toll-like receptor 4 (Tlr4) gene expression. Biochem J **2005**;387:355-65.
25. Ferrandino G, Nicola JP, Sanchez YE, Echeverria I, Liu Y, Amzel LM*, et al.* Na+ coordination at the Na2 site of the Na+/I- symporter. Proc Natl Acad Sci U S A **2016**;113:E5379-88.
26. Geraldo MV, Yamashita AS, Kimura ET. MicroRNA miR-146b-5p regulates signal transduction of TGF-beta by repressing SMAD4 in thyroid cancer. Oncogene **2012**;31:1910-22.
27. Knauf JA, Ma X, Smith EP, Zhang L, Mitsutake N, Liao XH*, et al.* Targeted expression of BRAFV600E in thyroid cells of transgenic mice results in papillary thyroid cancers that undergo dedifferentiation. Cancer Res **2005**;65:4238-45.
28. Nicola JP, Peyret V, Nazar M, Romero JM, Lucero AM, Montesinos Mdel M*, et al.* S-Nitrosylation of NF-kappaB p65 Inhibits TSH-Induced Na(+)/I(-) Symporter Expression. Endocrinology **2015**;156:4741-54.
29. Montesinos MM, Nicola JP, Nazar M, Peyret V, Lucero AM, Pellizas CG*, et al.* Nitric oxide-repressed Forkhead factor FoxE1 expression is involved in the inhibition of TSH-induced thyroid peroxidase levels. Mol Cell Endocrinol **2016**;420:105-15.
30. Li W, Nicola JP, Amzel LM, Carrasco N. Asn441 plays a key role in folding and function of the Na+/I-symporter (NIS). Faseb J **2013**;27:3229-38.
31. Rossich LE, Thomasz L, Nicola JP, Nazar M, Salvarredi LA, Pisarev M*, et al.* Effects of 2-iodohexadecanal in the physiology of thyroid cells. Mol Cell Endocrinol **2016**;437:292-301.
32. Plotnik JP, Budka JA, Ferris MW, Hollenhorst PC. ETS1 is a genome-wide effector of RAS/ERK signaling in epithelial cells. Nucleic Acids Res **2014**;42:11928-40.
33. Cancer Genome Atlas Research Network. Integrated genomic characterization of papillary thyroid carcinoma. Cell **2014**;159:676-90.
34. Xing M. Molecular pathogenesis and mechanisms of thyroid cancer. Nat Rev Cancer **2013**;13:184-99.
35. Kawai T, Akira S. Signaling to NF-kappaB by Toll-like receptors. Trends Mol Med **2007**;13:460-9.
36. Sizemore GM, Pitarresi JR, Balakrishnan S, Ostrowski MC. The ETS family of oncogenic transcription factors in solid tumours. Nat Rev Cancer **2017**;17:337-51.
37. Kim YH, Choi YW, Han JH, Lee J, Soh EY, Park SH*, et al.* TSH signaling overcomes B-RafV600E-induced senescence in papillary thyroid carcinogenesis through regulation of DUSP6. Neoplasia **2014**;16:1107-20.
38. de Nigris F, Mega T, Berger N, Barone MV, Santoro M, Viglietto G*, et al.* Induction of ETS-1 and ETS-2 transcription factors is required for thyroid cell transformation. Cancer Res **2001**;61:2267-75.
39. Shaikhibrahim Z, Lindstrot A, Langer B, Buettner R, Wernert N. Comprehensive gene expression microarray analysis of Ets-1 blockade in PC3 prostate cancer cells and correlations with prostate cancer tissues: Insights into genes involved in the metastatic cascade. Int J Mol Med **2011**;27:811-9.
40. Huang L, Yuan K, Liu J, Ren X, Dong X, Tian W*, et al.* Polymorphisms of the TLR4 gene and risk of gastric cancer. Gene **2014**;537:46-50.
41. Castano-Rodriguez N, Kaakoush NO, Mitchell HM. Pattern-recognition receptors and gastric cancer. Front Immunol **2014**;5:336.

42. Zheng SL, Augustsson-Balter K, Chang B, Hedelin M, Li L, Adami HO*, et al.* Sequence variants of toll-like receptor 4 are associated with prostate cancer risk: results from the CAncer Prostate in Sweden Study. Cancer Res **2004**;64:2918-22.
43. Slattery ML, Herrick JS, Bondurant KL, Wolff RK. Toll-like receptor genes and their association with colon and rectal cancer development and prognosis. Int J Cancer **2012**;130:2974-80.
44. Kim MK, Park SW, Kim SK, Park HJ, Eun YG, Kwon KH*, et al.* Association of Toll-like receptor 2 polymorphisms with papillary thyroid cancer and clinicopathologic features in a Korean population. J Korean Med Sci **2012**;27:1333-8.
45. Kim SK, Park HJ, Hong IK, Chung JH, Eun YG. A missense polymorphism (rs11466653, Met326Thr) of toll-like receptor 10 (TLR10) is associated with tumor size of papillary thyroid carcinoma in the Korean population. Endocrine **2013**;43:161-9.
46. Bohm J, Niskanen L, Tammi R, Tammi M, Eskelinen M, Pirinen R*, et al.* Hyaluronan expression in differentiated thyroid carcinoma. J Pathol **2002**;196:180-5.
47. Medapati MR, Dahlmann M, Ghavami S, Pathak KA, Lucman L, Klonisch T*, et al.* RAGE Mediates the Pro-Migratory Response of Extracellular S100A4 in Human Thyroid Cancer Cells. Thyroid **2015**;25:514-27.
48. Hoesel B, Schmid JA. The complexity of NF-kappaB signaling in inflammation and cancer. Mol Cancer **2013**;12:86.
49. Dhawan P, Richmond A. A novel NF-kappa B-inducing kinase-MAPK signaling pathway up-regulates NF-kappa B activity in melanoma cells. J Biol Chem **2002**;277:7920-8.
50. Plantinga TS, Petrulea MS, Oosting M, Joosten LAB, Piciu D, Smit JW*, et al.* Association of NF-kappaB polymorphisms with clinical outcome of non-medullary thyroid carcinoma. Endocr Relat Cancer **2017**;24:287-98.

FIGURES AND FIGURE LEGENDS

Figure 1. TLR4 is overexpressed in differentiated thyroid carcinomas. A. Representative normal and malignant thyroid sections showing TLR4 protein expression levels assessed by immunohistochemistry using a goat polyclonal anti-TLR4 antibody (sc-16240, Santa Cruz Biotechnology). Scale bar represents 20 µm. Quantification of TLR4 protein levels was expressed relative to the number of cells in the tissue sections and plotted as median with interquartile range. *** P<0.001 vs. normal tissue (Kruskal-Wallis test, Dunn's test). **B and C.** TLR4 protein expression in match-samples of tumor adjacent normal thyroid tissue and PTC, and match-samples of primary PTC and its lymph node metastasis. Scale bar represents 20 µm. * P<0.05 (Paired t test). **D.** Analysis of TLR4 mRNA expression as a function of the most frequent driver oncogenes identified in PTCs, including point mutations of BRAF (n=234), HRAS (n=14), and NRAS (n=34) genes, as well as fusions involving NTRK (n=10) and RET (n=32) tyrosine kinases, and BRAF (n=12) kinase. **E.** Correlative analysis showing TLR4 mRNA expression and ERK activation score in PTCs harboring oncogenes classically involved in MAPK/ERK signaling activation (n=336, Spearman's correlation test). ERK score was calculated based on a 52-gene signature to assess the MAPK/ERK signaling pathway activation (33). **F.** Correlative analysis showing TLR4 mRNA expression and thyroid differentiation score in PTCs harboring the oncogene $BRAF^{V600E}$ (n=234, Spearman's correlation test). Thyroid differentiation score was calculated based on a 16-gene signature related to thyroid metabolism and function (33). **G.** Correlative analysis showing TLR4 mRNA expression and MACIS score in PTCs harboring the oncogene $BRAF^{V600E}$ (n=212, Spearman's correlation test). **H.** Disease-free survival analysis of patients whose thyroid tumors harbored the oncogene $BRAF^{V600E}$ (wild-type TERT status) and expressed low (n=97) or high (n=88) TLR4 mRNA levels, based on its expression below and above the median within the group. P=0.0071 (Mantel-Cox test).

Figure 2. Conditional oncogene expression induced TLR4 expression in PTC models. A. RT/qPCR assessing TLR4 mRNA expression levels in response to doxycycline (Dox)-induced $BRAF^{V600E}$, $HRas^{G12V}$, or RET/PTC3 expression at 48 h in PCCl3 cells. * P<0.05 and ** P<0.01 vs. vehicle-treated cells (one-way ANOVA, Newman-Keuls test). **B and C.** Immunoblot assessing TLR4 protein expression levels in response to conditional $BRAF^{V600E}$ expression for 48 h in PC/BRAF cells **(B)** or transient transfection of $BRAF^{V600E}$ into non-tumoral Nthy-ori 3-1 thyroid cells **(C)**. Fold change indicates relative TLR4 abundance. * P<0.05 vs. vehicle-treated cells or empty vector-transfected cells (unpaired Student's t test). **D.** Immunofluorescence under non-permeabilized conditions analyzing TLR4 protein expression at the plasma membrane in response to $BRAF^{V600E}$ expression for 48 h in PC/BRAF cells. Scale bar represents 10 µm. *** P<0.001 vs. vehicle-treated cells (unpaired Student's t test). **E and F.** Analysis of TLR4 mRNA and protein expression in the thyroid tissue of transgenic mice conditionally expressing $BRAF^{V600E}$ in the thyroid follicular cell and littermate control mice. Scale bar represents 20 µm. Quantification of TLR4 protein expression was expressed relative to the numbers of cells in the tissue sections. * P<0.05 and ** P<0.001 (Mann Whitney t test).

Figure 3. TLR4 signaling in PTC cell models. A. NF-κB reporter activity in doxycycline (Dox)-treated $PC/BRAF^{V600E}$ cells stimulated with the exogenous TLR4-agonist LPS. The NF-κB inhibitor BAY 11-7082 is used as specificity control. *** P<0.001 vs. vehicle-treated cells, $^{\#}$ P<0.05 vs. Dox-treated cells in the absence of LPS, $^{\#\#}$ P<0.01 and $^{\#\#\#}$ P<0.001 vs. Dox-treated cells (one-way ANOVA, Newman-Keuls test). **B and C.** RT/qPCR assessing the mRNA expression of the NF-κB targets IL-6 and iNOS in response to TLR4 activation for 12 h. ** P<0.01 and *** P<0.001 vs. vehicle-treated cells, $^{\#\#\#}$ P<0.001 vs. LPS-treated cells (one-way ANOVA, Newman-Keuls test). **D.** NF-κB reporter activity in empty or non-signaling TLR4 or MyD88

vectors-transfected BCPAP cells stimulated with LPS for 24 hs. Empty vector-transfected cells treated with BAY 11-7082 serves as specificity control. ** P<0.01 vs. vehicle-treated cells, ## P<0.01 and ### P<0.001 vs. LPS-treated empty vector-transfected cells (one-way ANOVA, Newman-Keuls test). **E and F.** RT/qPCR assessing the mRNA expression of IL-6 and iNOS in BCPAP cells stimulated with LPS for 12 hs. *** P<0.001 vs. vehicle-treated cells, ### P<0.001 vs. LPS-treated cells (one-way ANOVA, Newman-Keuls test).

Figure 4. MAPK/ERK signaling regulates TLR4 gene expression in response to BRAF^{V600E}. A and B. TLR4 protein and mRNA expression in doxycycline-treated PC/BRAF^{V600E} cells in the presence of the chemical inhibitors PLX4032 or U0126. Fold change indicates relative TLR4 abundance. * P<0.05 and ** P<0.01 vs. vehicle-treated cells, # P<0.05 vs. same condition in absence of inhibitor (one-way ANOVA, Newman-Keuls test). **C and D.** TLR4 protein and mRNA expression in BCPAP cells treated in the presence of the chemical inhibitors PLX4032 or U0126. Fold change indicates relative TLR4 abundance. * P<0.05 and ** P<0.01 vs. vehicle-treated cells (one-way ANOVA, Newman-Keuls test).

Figure 5. Ets^{d} binding site is crucial for TLR4 gene transcription in response to constitutive BRAF^{V600E} signaling. A. Transcriptional activity of TLR4 promoter deletion constructs in response to BRAF^{V600E} expression in PC/BRAF^{V600E} cells. * P<0.05 and *** P<0.001 vs. vehicle-treated cells (unpaired Student's t test). **B.** Transcriptional activity of the Ets^{d} binding-site mutated TLR4 promoter construct -336/+223 in PC/BRAF^{V600E} cells. *** P<0.001 vs. vehicle-treated cells, ### P<0.001 vs. -336/+223-transfected cells (one-way ANOVA, Newman-Keuls test). **C.** Transcriptional activity of the trimeric Ets^{d} reporter construct 3x Ets^{d}-Luc in PC/BRAF^{V600E} cells in response to doxycycline (Dox) treatment. * P<0.05 (unpaired Student's t test). **D.** Transcriptional activity of the TLR4 promoter construct -336/+223 and Ets^{d} binding-site mutated TLR4 promoter construct -336/+223 in BCPAP cells. ** P<0.01 vs. -336/+223-transfected cells (unpaired Student's t test).

Figure 6. ETS1 mediates BRAF^{V600E}-induced TLR4 gene expression. A. Correlation analysis of TLR4 mRNA expression as a function of ETS1 mRNA expression in the subset of PTC harboring the oncogene BRAF^{V600E} (n=234, Spearman's correlation test). **B.** Representative unmatched sections of normal thyroid tissue and PTC showing ETS1 protein expression levels assessed by immunohistochemistry using a rabbit polyclonal anti-ETS1 antibody (sc-350, Santa Cruz Biotechnology). Scale bar represents 20 µm. Quantification of ETS1 protein levels was expressed relative to the number of cells in the tissue sections and plotted as median with interquartile range. *** P<0.001 vs. normal tissue (Mann Whitney test). **C.** Correlation analysis of TLR4 and ETS1 protein expression assessed by immunohistochemistry in equivalent PTC tissues (n=24, Spearman's correlation test). **D.** Immunoblot analysis assessing nuclear ETS1 protein levels in response to BRAF^{V600E} expression in PC/BRAF^{V600E} cells. PARP-1 and α-Tubulin were used as nuclear and cytoplasmic loading markers, respectively. Fold change indicates relative ETS1 abundance. * P<0.05 (unpaired Student's t test). **E.** Immunofluorescence analysis under permeabilized conditions showing ETS1 protein expression in response to doxycycline (Dox) treatment in PC/BRAF^{V600E} cells. Scale bar represents 10 µm. * P<0.05 (unpaired Student's t test). **F and G.** MAPK/ERK-dependent ETS1 protein expression in response to BRAF^{V600E} oncogenic activity in PC/BRAF^{V600E} and BCPAP cells. Fold change indicates relative ETS1 abundance. * P<0.05 vs. vehicle-treated cells (one-way ANOVA, Newman-Keuls test). **H.** Immunoblot analysis showing ETS1 protein expression in scramble (SCR) or ETS1 siRNA transfected PC/BRAF^{V600E} cells. Fold change indicates relative ETS1 abundance. * P<0.05 (unpaired Student's t test). **I.** TLR4 mRNA expression in doxycycline (Dox)-treated scramble (SCR) or ETS1 siRNA-transfected PC/BRAF^{V600E} cells. **

721 *P*<0.01 vs. vehicle-treated cells, ## *P*<0.01 vs siSCR-transfected cells (one-way ANOVA, Newman-Keuls test).
722 **J.** Transcriptional activity of the TLR4 promoter construct -336/+223 in doxycycline (Dox)-treated scramble
723 (SCR) or ETS1 siRNA-transfected PC/BRAF^{V600E} cells. * *P*<0.05 (one-way ANOVA, Newman-Keuls test). **K.**
724 Immunoblot analysis showing TLR4 protein expression in empty or ETS1 expressing vector-transfected
725 normal PCCl3 cells. Fold change indicates relative TLR4 abundance. * *P*<0.05 (unpaired Student's t test). **L.**
726 Transcriptional activity of the TLR4 promoter construct -336/+223 in empty or ETS1 expressing vector-
727 transfected normal PCCl3 cells. ** *P*<0.01 (unpaired Student's t test). **M.** ChIP analysis assessing ETS1
728 binding to TLR4 promoter region -365 to -24 (relative to the transcription start site) in response to BRAF^{V600E}
729 induction in PC/BRAF^{V600E} cells. ** *P*<0.01 vs. vehicle-treated cells (unpaired Student's t test).

FIGURE 1

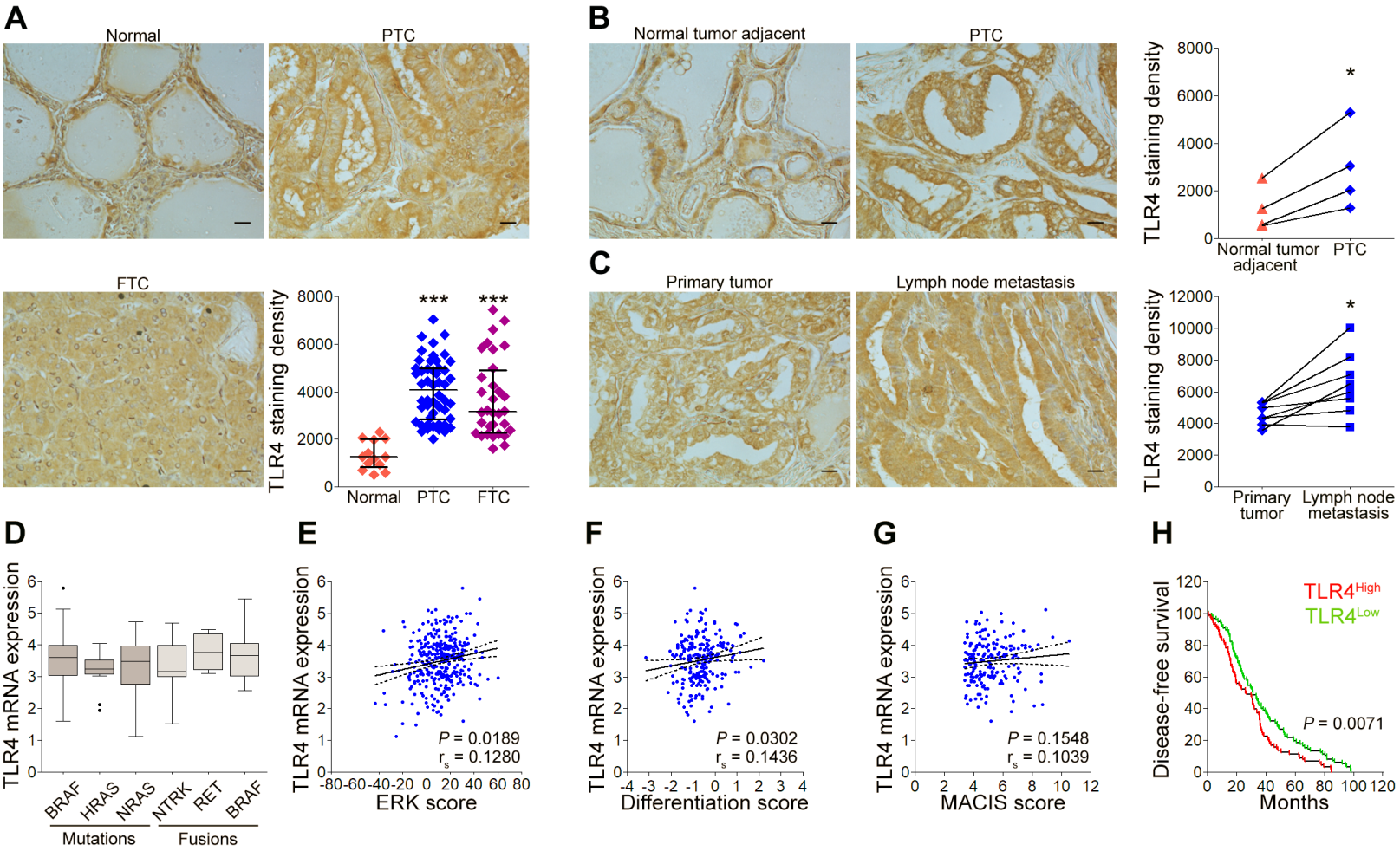

FIGURE 2

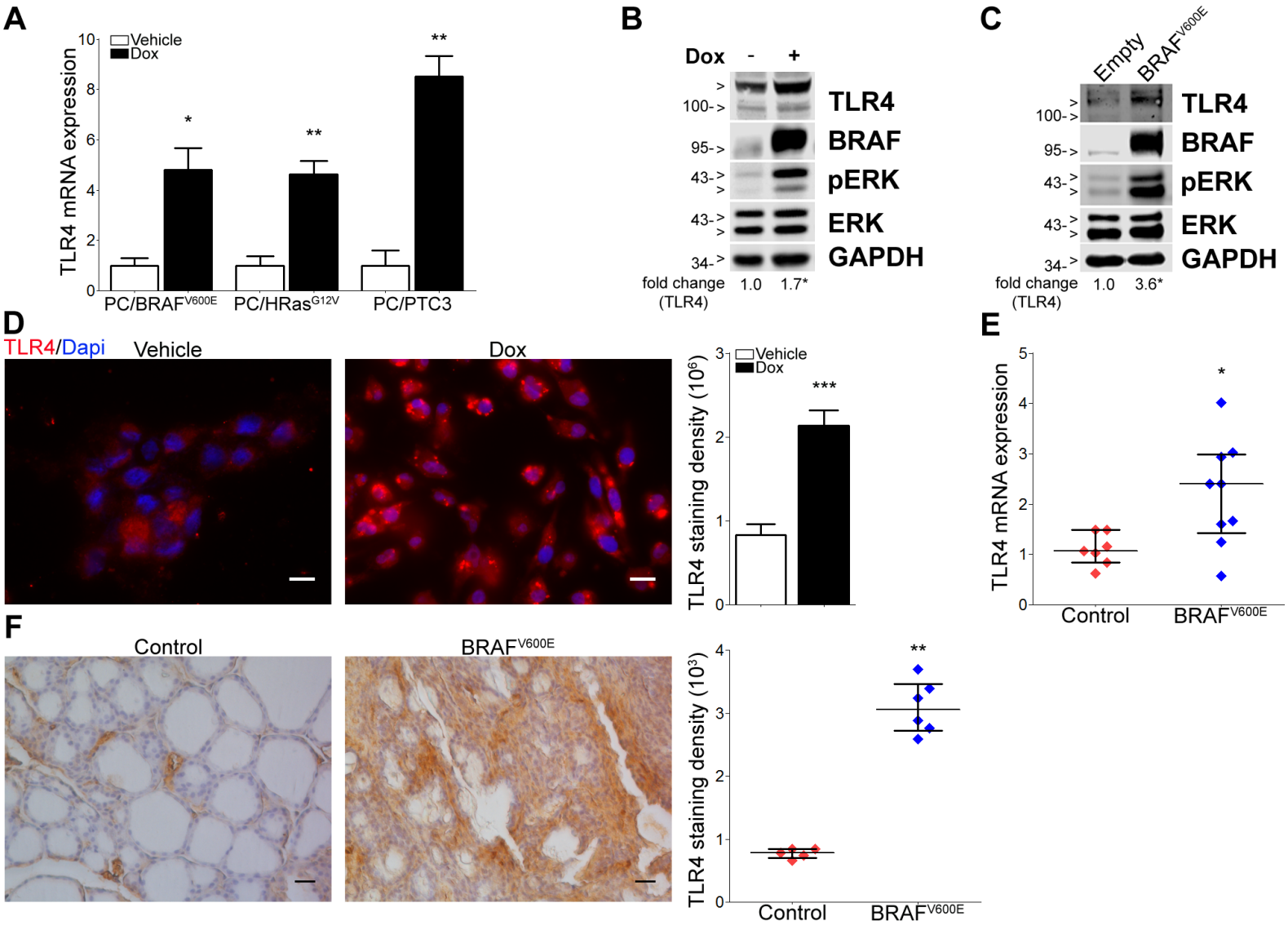

FIGURE 3

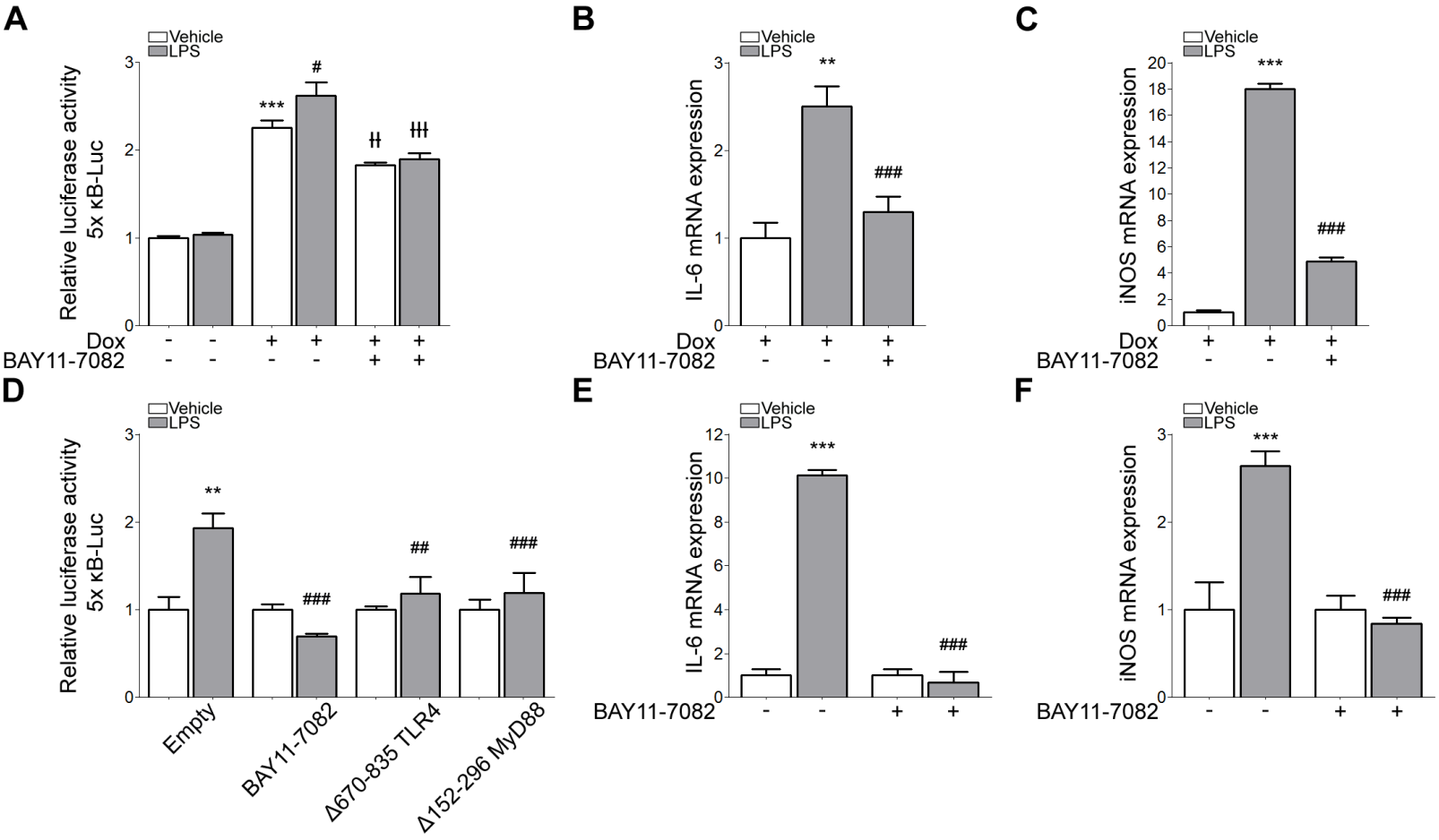

FIGURE 4

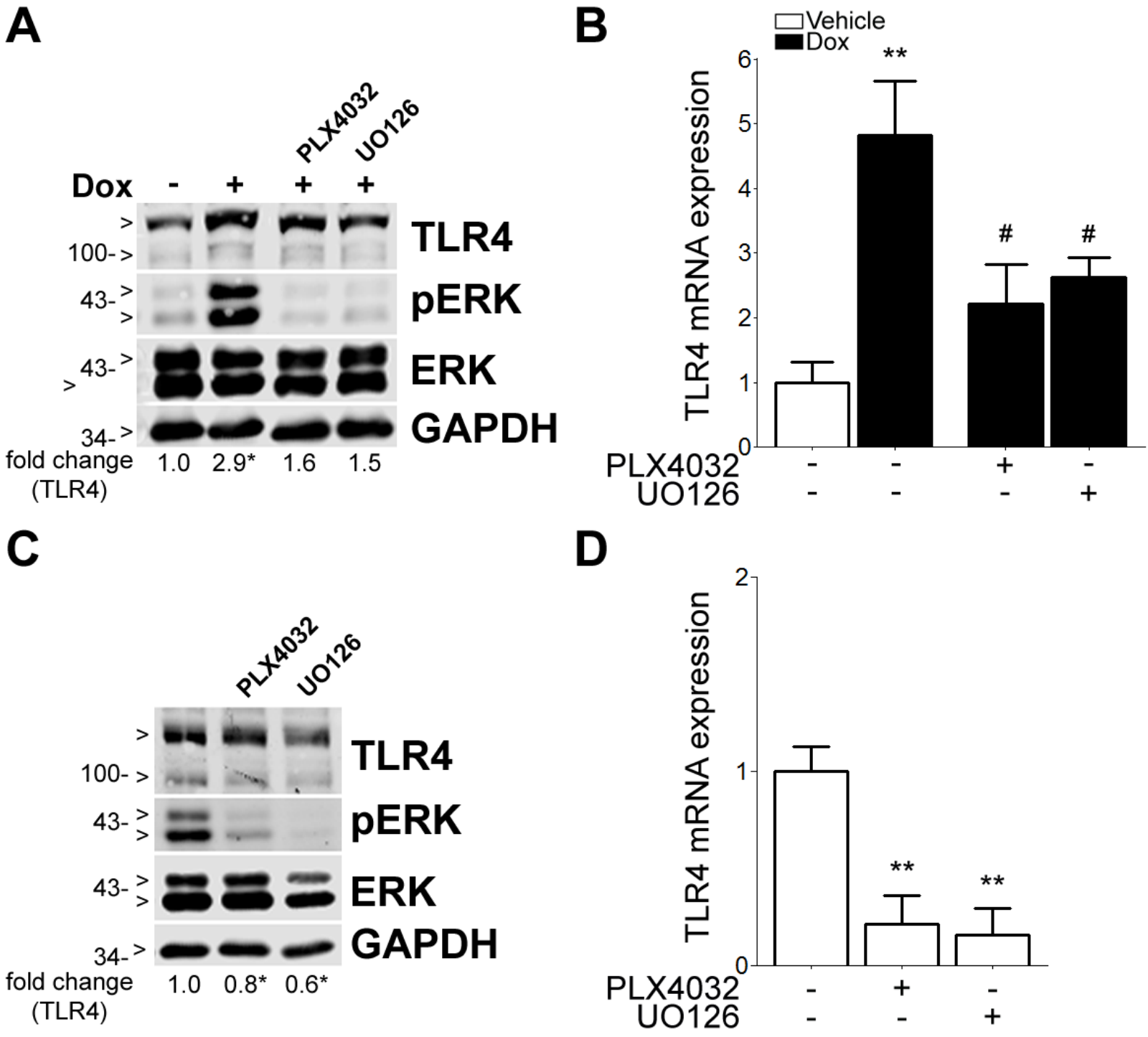

FIGURE 5

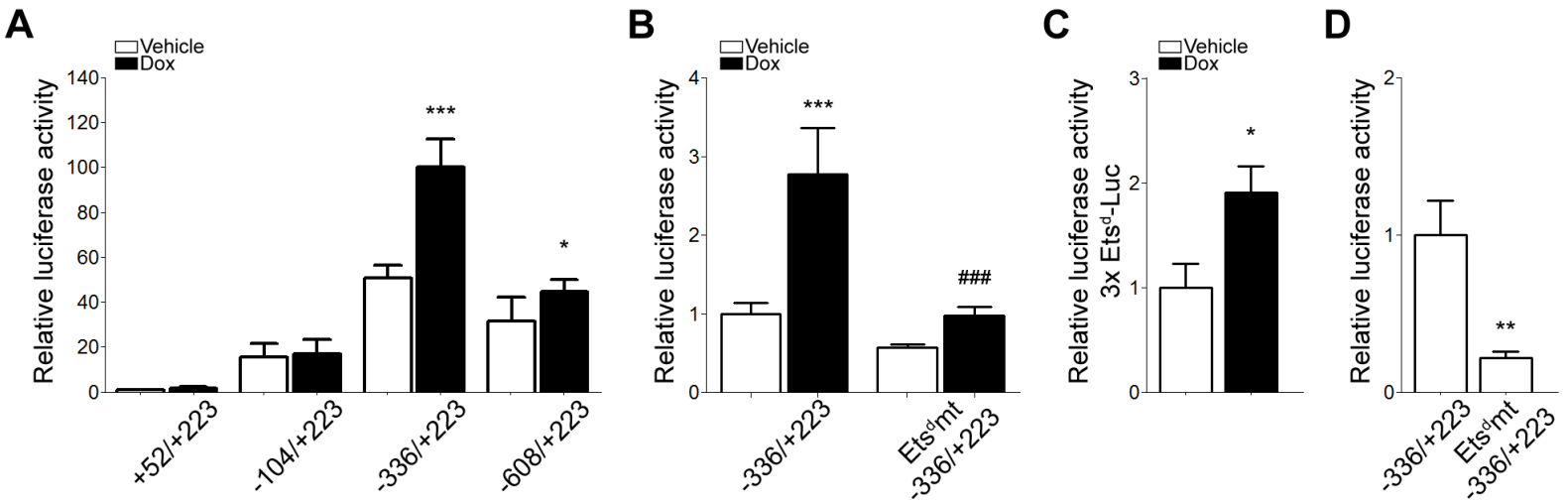

FIGURE 6

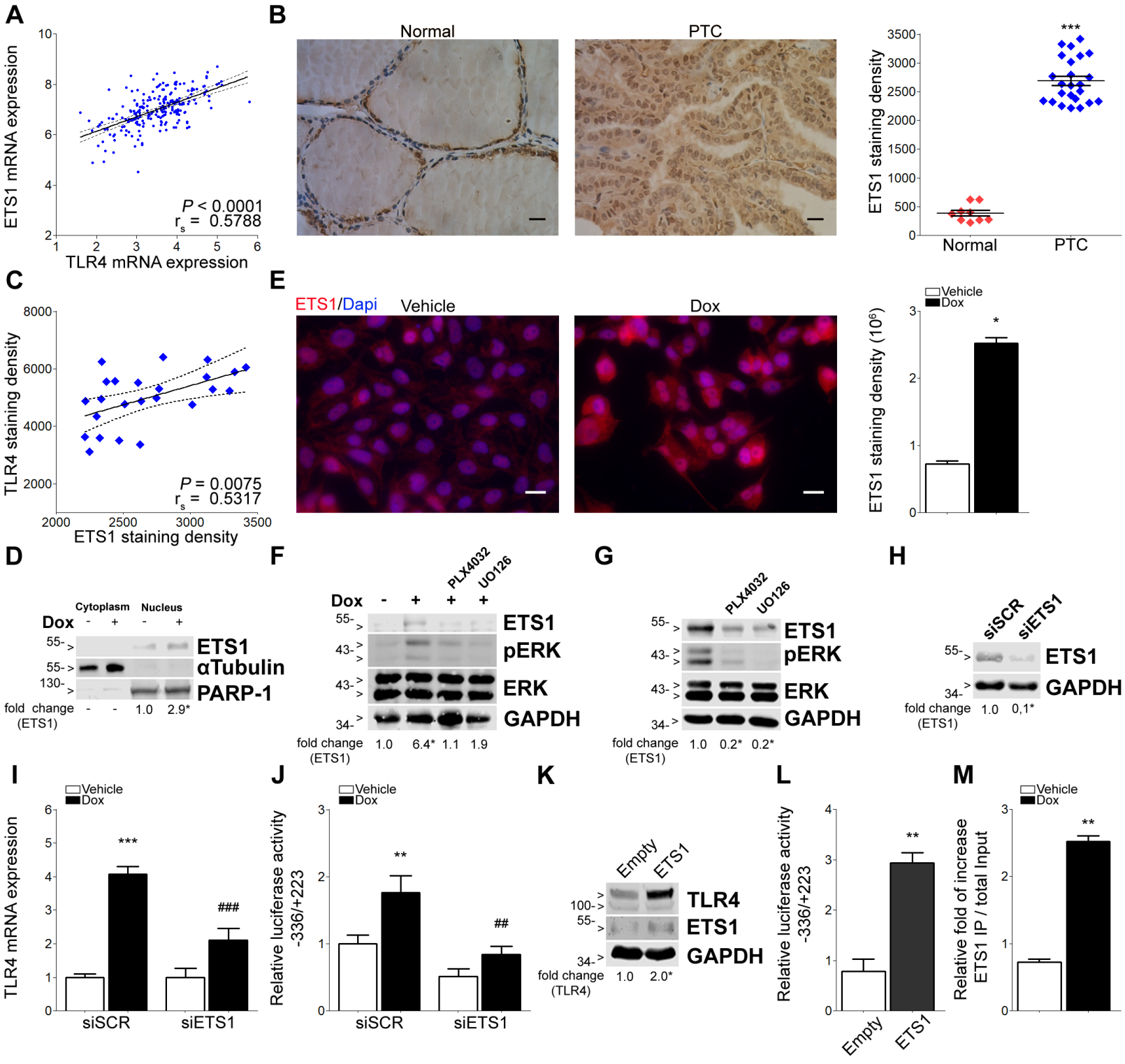

AACR American Association for Cancer Research

Molecular Cancer Research

Functional Toll-like Receptor 4 Overexpression in Papillary Thyroid Cancer by MAPK/ERK-induced ETS1 Transcriptional Activity

Victoria Peyret, Magalí Nazar, Mariano Martin, et al.

Mol Cancer Res Published OnlineFirst March 9, 2018.